RSC Advances

PAPER

View Article Online
View Journal | View Issue

Cite this: *RSC Adv.*, 2024, **14**, 5577

ROS-responsive polyprodrug micelles carrying suicide genes in combination with chemotherapy and gene therapy for prostate cancer treatment†

Kai Li, Sinan Tian, Ke Sun, Qingguo Su, Yanhui Mei and Wenjie Niu *

Received 14th January 2024
Accepted 8th February 2024

DOI: 10.1039/d4ra00352g

rsc.li/rsc-advances

Prostate cancer is the most common malignant tumor in the male reproductive system, and its incidence increases with age. Chemotherapy is one of the main strategies for treating prostate cancer, but it often comes with unavoidable side effects. Nanocarriers can improve drug utilization and targeting, and cationic carriers can also carry nucleic acids for gene therapy. In this study, we prepared a cationic micelle constructed from a polyprodrug that can deliver both chemotherapeutic drugs and nucleic acids simultaneously. The typical chemotherapeutic drug hydroxycamptothecin (HCPT) was linked by reactive oxygen species (ROS)-responsive coupling agents and forms amphiphilic block polymers with low molecular weight polyethyleneimine (PEI). The resulting cationic micelles can be triggered by high levels of ROS in tumor cells and collapse to release HCPT and suicide genes to kill tumor cells. At the same time, it reduces the killing of normal cells. In prostate cancer cells, it has been confirmed that the co-delivery carriers combined with chemotherapy and a suicide gene prodrug system have shown an ideal therapeutic effect on prostate cancer.

Introduction

Prostate cancer (PC) usually progresses slowly and the early symptoms are not obvious, so most patients are already in the middle or late stage at the initial diagnosis.[1–3] Therefore, PC is known as the number one "hidden killer" that endangers male life. At present, the main treatment methods for PC include surgery, radiotherapy, low-temperature surgery, chemotherapy, and endocrine therapy.[4–6] Among them, chemotherapy is suitable for patients who have developed metastases or have low responsiveness to hormone therapy. Commonly used chemotherapeutic drugs for PC include methotrexate, cyclophosphamide, and 5-fluorouracil (5-FU).[7–9] Due to the non-specific killing effect of clinical chemotherapeutic drugs, there will be some side effects on the patient's body, mainly manifested as bone marrow suppression, appetite loss, muscle pain, and fatigue.[10,11] Therefore, strengthening the targeting of chemotherapeutic drugs to the lesion site, so that chemotherapeutic drugs only play a role in the lesion site can develop the efficacy and moderate the toxic side effects on normal tissues.

Drug delivery systems can improve the solubility, bioavailability, and stability of drugs, and the targeted delivery and controlled release of drugs can be achieved. At present, a wide variety of nanocarriers have been reported, such as polymer nanoparticles, liposomes, and nonmetals/metal nanoparticles.[12–14] Some carriers can also be endowed with imaging or other functions to achieve integrated diagnosis and treatment.[15–17] Many chemotherapeutic drug molecules have active groups, such as amino and hydroxyl groups, which can be linked by condensation polymerization to obtain polymer prodrugs. Polyprodrugs can be used as hydrophobic segments and connect with hydrophilic polymers to form amphiphilic polymers. These amphiphilic polymer prodrugs can form micelles in aqueous solution.[18,19] A series of tumor microenvironment-responsive nanocarriers have been constructed based on biochemical indicators in tumor tissues that are different from normal tissues, for instance a slightly acidic environment and high levels of reactive oxygen species (ROS)/glutathione (GSH).[20,21] For example, Wang *et al.* exploited the nature that disulfide bonds can be broken by GSH to create a library of GSH-responsive silica nanocapsules for brain-targeted delivery of biologics *via* systemic administration.[22] These kinds of carriers have significant advantages in achieving tumor targeting, drug controlled release, and reducing unexpected toxic side effects during chemotherapy.

Gene therapy, an emerging method of cancer treatment, refers to the insertion of foreign genes into applicable recipient cells of patients by gene transfer technology, consequently the products produced by foreign genes can treat certain diseases.[23] The gene vector is the key for the foreign target gene to enter the host cell, which directly affects the therapeutic effect.[24,25] Gene vectors embrace viral vectors and non-viral vectors. The viral

Department of Urology, Binzhou Medical University Hospital, Binzhou, Shandong, 256500, P. R. China. E-mail: Dr_nwj327@bzmc.edu.cn

† Electronic supplementary information (ESI) available: The ^{1}H-NMR spectrums of ROS-responsive coupling agent, TK-pHCPT and HD-pHCPT. See DOI: https://doi.org/10.1039/d4ra00352g

vector has great transfection efficiency and targeting specificity, but it also has safety problems such as high immunogenicity and bottlenecks in large-scale production.[26] Relatively, although the transfection efficiency of non-viral vectors is not as good as that of viral vectors, non-viral vectors have low immunogenicity, high safety, large capacity for carrying foreign target genes, simple operation, and low cost.[25] Due to breakthroughs in nanotechnology, precise design of non-viral gene vectors can also be achieved.

In this study, a ROS-responsive coupling agent was prepared to link hydroxycamptothecine molecules (HCPT) together through condensation polymerization. A low molecular weight cationic polymer PEI (M_W = 1800 Da) was subsequently grafted to the end of the polyprodrug (pHCPT), and the resulting amphiphilic block copolymer could self-assemble into nanomicelles in an aqueous solution, as shown in Fig. 1. The cationic shell of the micelle can chelate suicide genes. The CD/5-FC (cytosine deaminase/5-fluorocytosine) suicide gene/prodrug system can effectively kill tumor cells through direct toxic effects and bystander effects.[27,28] 5-FU, an anti-pyrimidine drug, is a generally used chemotherapeutic drug for PC therapy and has a good effect on solid tumors.[29,30] If 5-FU is injected intravenously, there will be significant gastrointestinal reactions, such as nausea, vomiting, and diarrhea, and may be accompanied by bone marrow suppression. However, mammalian cells do not contain the CD gene, so a gene vector is used to transfer the CD suicide gene (pCMV-CD) to tumor cells, and then low-toxicity precursor chemotherapeutic drug 5-FC is injected systemic or locally. Under the action of cytosine deaminase expressed by the CD gene, 5-FC is deaminated and converted into toxic 5-FU. Only when triggered by high levels of ROS in tumor cells can HCPT and suicide genes be released efficiently. PC cells are effectively killed by a combination of chemotherapy and gene therapy, while normal cells are spared damage.

Results and discussion

Characterization of the micelles and micelle/pDNA complexes

The preparation of polyprodurg segments was referred to the reported methods.[18] A coupling agent containing a thioketal structure was first prepared. With the help of triphosgene,

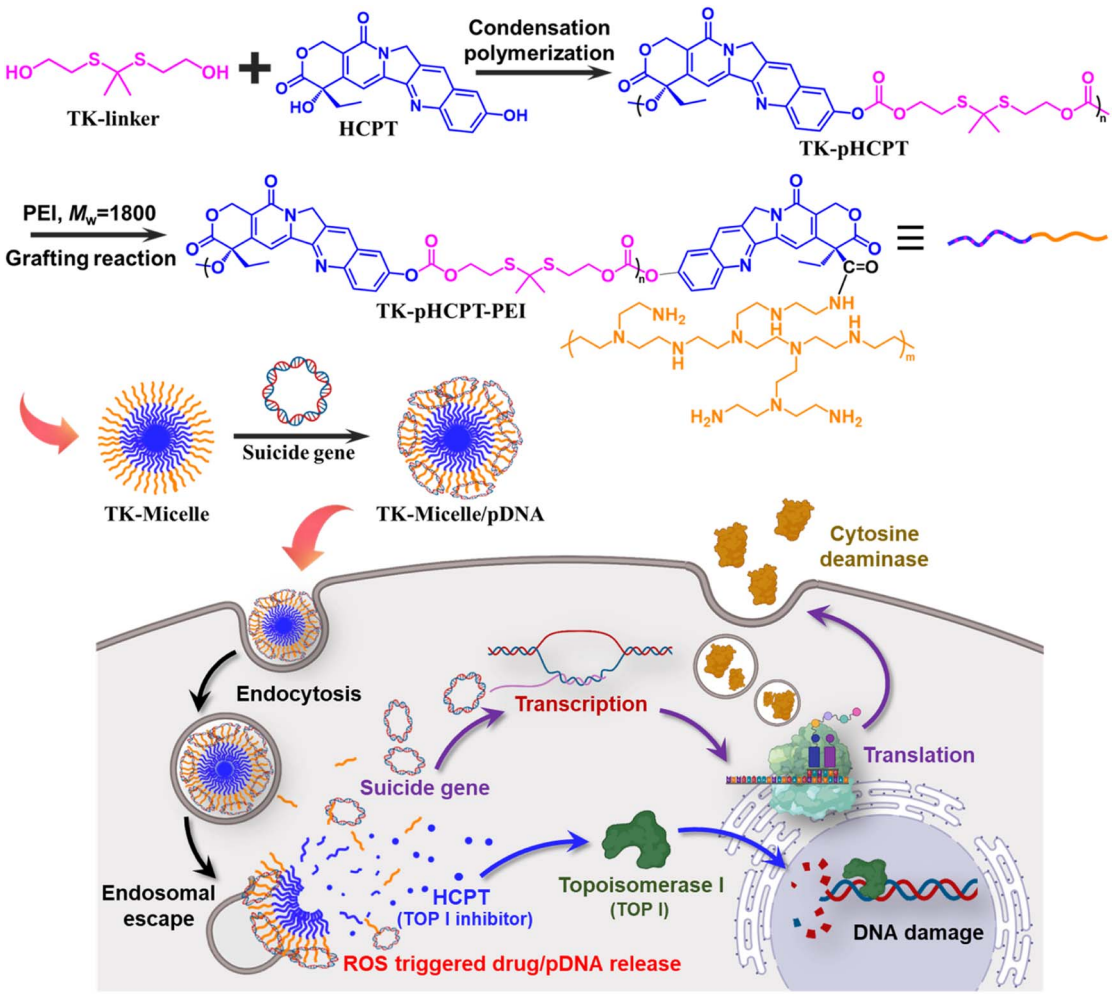

Fig. 1 Schematic diagram demonstrating the synthesis process of polyprodrugs and the controlled release of HCPT and suicide genes triggered by high levels of ROS in PC cells.

HCPT molecules were joined together by hydroxyl groups on the coupling agent to form the polyprodurg (termed as TK-pHCPT). The synthesis process is presented in Fig. 1. The appearance of characteristic peaks in the ^{1}H NMR spectra confirms the successful synthesis of the compounds (Fig. S1 and S2†). The molecular weight (M_W) of the polyprodurg is about 4500 Da (Fig. S3†). Subsequently, the residual hydroxyl group at the end of the polyprodurg chain was activated by 1,1′-carbonyldiimidazole (CDI) and further reacted with the amino group of PEI ($M_W = 1800$ Da) to form amphiphilic polymers (TK-pHCPT-PEI, yield ~74.9%, $M_W = 10\,300$ Da). The control group without ROS-responsive (termed as HD-pHCPT) was prepared by polycondensation using 1,7-heptanediol as a coupling agent (Fig. S4 and S5†). The content of HCPT in polyprodurgs is about 31%.

The resulting amphiphilic polymers TK-pHCPT-PEI and HD-pHCPT-PEI were dissolved in a small amount of DMSO and then slowly added to an appropriate amount of PBS buffer. The micelle was obtained after stirring. The micelles with ROS responsiveness are called TK-Micelle, while the control group without responsiveness is called HD-Micelle. Polycations can form complexes with negatively charged plasmids through electrostatic interactions.[25] The size and tightness of the complex are influenced by the amount of cationic charge. These cationic micelles serve as gene carriers, and their performance in compressing plasmids was evaluated through agarose gel electrophoresis. The ratio of positive and negative charges is expressed by the nitrogen–phosphorus ratio (N/P ratio). Positive charge comes from PEI with ionizable ammonium ions (N), while negative charge comes from nucleic acid molecules with phosphate ions (P).[31] The loading capacity, particle size, stability, and biocompatibility of the complex are affected by the N/P ratio. As shown in Fig. 2, both cationic micelles can capture the plasmid well when the N/P ratio is between 1 and 1.5. In the presence of hydrogen peroxide, bright bands can still be observed until the N/P ratio reach 2.5. Hydrogen peroxide is a major form of ROS present in cells.[20] We speculate that hydrogen peroxide causes the cleavage of the thioketal structure and further leads to the disintegration of micelles. Incomplete micelles cannot effectively compress plasmids, resulting in plasmid migration under the action of an electric field.

Transmission electron microscopy (TEM) images (Fig. 3a) clearly show the morphology of TK-Micelle. The micelles are spherical and uniformly dispersed with a particle size of less than 100 nm. After complexing with the plasmid, the particle size of the complex decreased and became more uniform (Fig. 3b). This is because the interaction between charges makes the nanoparticles more compact. When 50 μM of hydrogen peroxide is added to the complex, the structure of the micelle is obviously observed to be destroyed (Fig. 3c). It was again confirmed that the micelles had ROS-responsive properties.

The particle size of cationic micelle/pDNA complexes at varying N/P ratios is shown in Fig. 3d. At the N/P ratio of 5, the particle size of the complexes formed by the cationic micelles and plasmids reached 130 nm. We speculated that this was because insufficient cations were unable to condense the plasmids effectively, and only adsorbed the plasmids around the micelles to form a loose structure. With the upturn of the N/P ratio, the particle size of the complex gradually decreases and stabilizes at around 60 nm. Nanocarriers with a particle size of not more than 100 nm can be effectively internalized by cells, thus facilitating the transport of drugs and nucleic acids.[32] The particle size of PEI/pDNA complexes was larger than that of micelle/DNA complexes within the testing range.

The zeta-potential of micelles and complexes is shown in Fig. 3e. The surface potential of cationic micelles is around 43 mV. At low N/P ratios, the negative charge of plasmids shields part of the positive charge, which reduces the potential of the complex. With the increase of cationic micelle quantity, the zeta-potential increases and approaches the surface potential of pure micelle. The surface positivity is beneficial for the contact between the nanocarrier and the cell membrane. However, it should be recognized that excessive positive charges may cause destruction to the cell membrane and need to be comprehensively evaluated. The carrier should maintain sufficient stability during storage and internal circulation. After being placed in PBS for a week, it was found that the particle size of TK-Micelles increased from the third day, but remained around 100 nm, while the particle size of HD-Micelles remained relatively stable (Fig. 3f).

Characterization of the ROS-responsive behavior

The thioketal structure will break in high concentrations of ROS, enabling controlled release of the original HCPT drug molecule. It has been stated that the concentration of ROS in tumor cells reaches 50–100 $\times$ 10^{-6} M.[33] Drug release triggered by high ROS levels within tumor cells was simulated (Fig. 4). In the absence of hydrogen peroxide, TK-Micelles are barely released during the testing time. After adding hydrogen peroxide with a concentration of 50 μM, it can be detected that HCPT was released in the early stage, and the release reached the limit in nearly 48 h. Due to the non-responsiveness of HD-

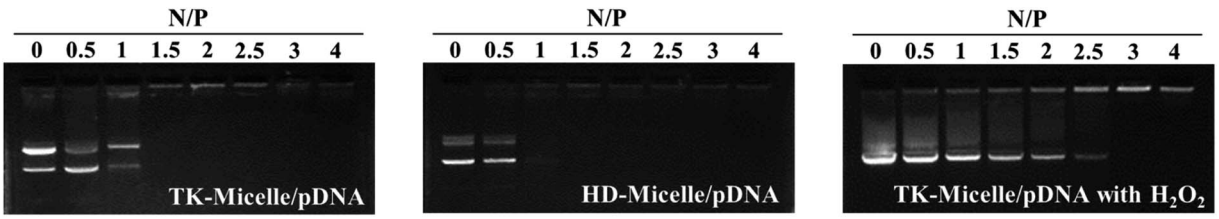

Fig. 2 The agarose gel electrophoresis of the TK-Micelle/pDNA, HD-Micelle/pDNA, and TK-Micelle/pDNA with H_2O_2 (50 μM) at various N/P ratios.

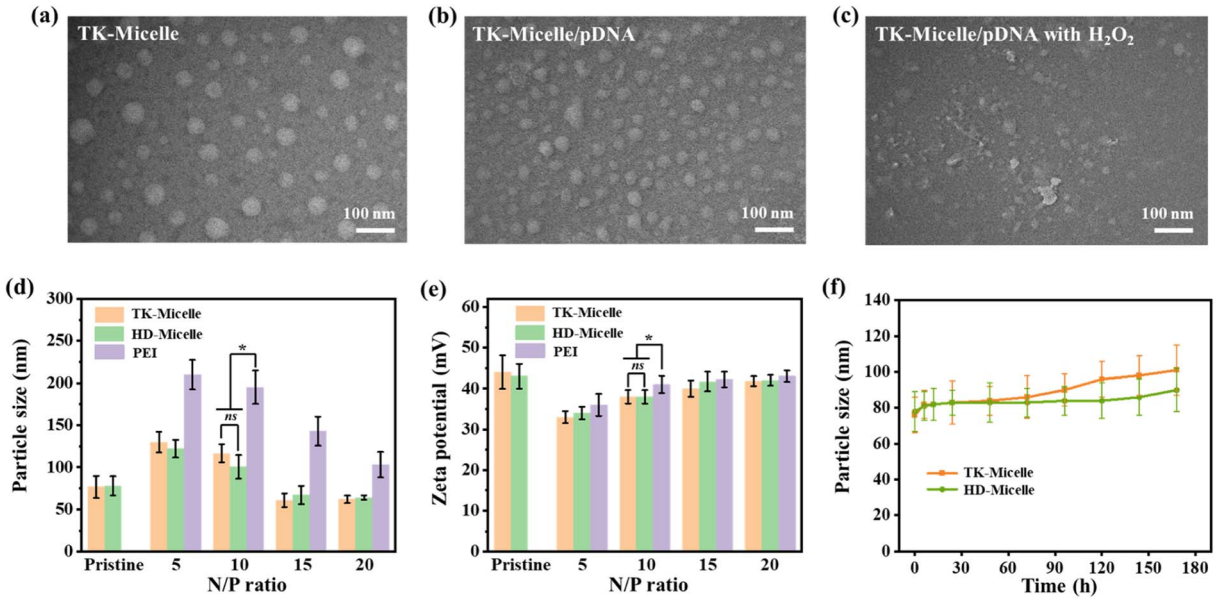

Fig. 3 TEM images of the (a) TK-Micelles, (b) TK-Micelle/pDNA complexes (N/P = 15), and (c) TK-Micelle/pDNA complexes (N/P = 15) with H_2O_2 (50 μM). The (d) particle size and (e) zeta potential of TK-Micelles, HD-Micelles, PEI, and their complexes at different N/Ps. (f) The change in particle size of the TK-Micelle and HD-Micelle diffused in PBS (pH = 7.4) for 14 days. Mean ± s.d., $n = 3$, *$p < 0.05$.

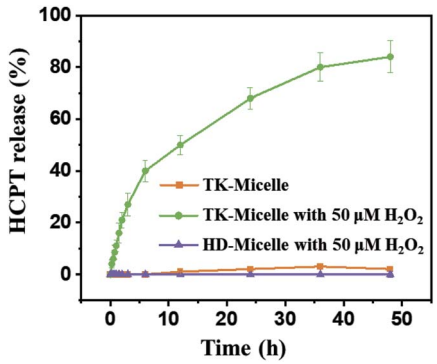

Fig. 4 The release profile of HCPT released from TK-Micelles, TK-Micelles with 50 μM H_2O_2, and HD-Micelles with 50 μM H_2O_2. Mean ± s.d., $n = 3$.

Micelles, even in the presence of hydrogen peroxide, significant release of HCPT cannot be detected. This ROS-responsive release behavior is conducive to the rapid release of chemotherapeutic drugs and nucleic acids in tumor cells, and to a certain extent, avoids damage to normal cells.

Blood compatibility of carriers. Nanocarriers need to travel through blood circulation to reach the tumor site. Therefore, good blood compatibility is a pre-condition for *in vivo* utilization of carriers. Making chemotherapeutic drugs into polymer and encapsulating them inside micelles can reduce the adverse effects. The PEI segments outside the micelles are hydrophilic cationic polymers. It is generally believed that cationic polymers may interact with the red blood cell (RBC) membrane through electrostatic interactions, leading to the rupture of RBCs and causing hemolysis.[34] Therefore, the blood compatibility of the prepared micelles was evaluated by hemolysis tests. As shown in Fig. 5a and b, no significant hemolysis was observed even while the concentration of micelles extended to 200 μg mL^{-1} or the N/P reached 20, and the hemolysis rate was below 1% (Fig. 5c). We speculate that this is because of the small molecular weight of PEI used to construct the carrier. The molecular weight of PEI applied is 1800 Da, which is much lower than the molecular weight of PEI commonly used as a transfection reagent (M_W = 25 000 Da). The low surface charge density ensures that the prepared micelles have good blood compatibility. When the micelles were complexed with the plasmid, the hemolysis rate was further reduced (Fig. 5d). This may be due to the plasmids on the surface of the nanocarriers shielding a portion of the surface positive charge. It should be noted that for cationic polymers, biocompatibility and the ability to condense nucleic acids are contradictory. A high density of positive charge makes it easier and more efficient to condense nucleic acids, but at the same time, it brings higher cytotoxicity. Fortunately, the carrier we have prepared achieved an ideal balance between these two properties.

The internalization efficiency of carriers

Effective uptake of nanocarriers by cells can ensure that the required amount of drugs is achieved internally. We labeled plasmid (pRL-CMV) using a green fluorescent probe (YOYO-1). PEI with a molecular weight of 25 000 Da is considered as the gold standard of transfection, and the supreme transfection efficiency is achieved when the N/P ratio is 10.[35] The ROS-responsive micelle was complexed with the labeled plasmid to achieve an N/P ratio of 10. The fluorescence intensity of positive cells was quantified by flow cytometry. As shown in Fig. 6, the internalization rate of TK-Micelle/pDNA complexes was 87.6%. This indicates that micelles can effectively transport plasmids

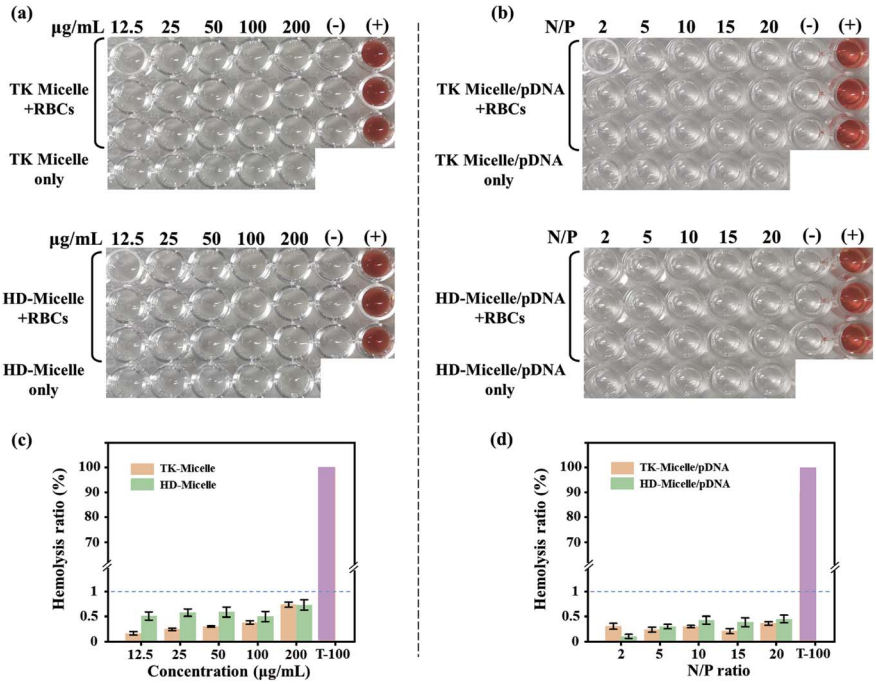

Fig. 5 The hemolysis assessment of (a) micelles and (b) micelle/pDNA complexes (−: negative control; +: positive control; concentration of micelles or N/P ratio). Hemolysis rate of (c) micelles and (d) micelle/pDNA complexes. Mean ± s.d., $n = 3$.

into cells. The phosphoric acid group on the lipid bilayer of the cell membrane is negatively charged, thus positively charged carriers can be bonded to the cell membrane by electrostatic action, thus facilitating the internalization process of the cell. The introduction of ROS-sensitive bonds does not affect the internalization process of micelles towards cells.

Cytotoxicity of micelles constructed by polyprodrugs

To evaluate the efficacy of the polyprodrug, we evaluated the ability of micelles and free HCPT to kill 22RV1 cells and L929 cells using standard MTT assay (Fig. 7). The 22RV1 cell line is human PC cells, while the L929 cell line used as the control group is mouse epithelial fibroblasts. Generally, all groups showed more effective killing of 22RV1 cells, especially at high concentrations. This may be related to the more active replication of cancer cells compared to normal cells. The anticancer mechanism of HCPT mainly interferes with the DNA replication of tumor cells through topoisomerase I (Topo I), thus inhibiting the growth of tumor cells.[36] TK-Micelles showed lower cell survival in 22RV1 cells with a half-maximal inhibition concentration (IC50) of 62.4 μg mL^{-1}. This is because cancer cells have higher levels of ROS, which allows the thioketal structure between the HCPT molecules to rapidly broken in response, thereby decomposing into active pharmaceutical molecules and exerting therapeutic effects. However, the cell viability of L929 cells was higher than that of 22RV1 cells at the same concentration owing to the low concentration of ROS and the slow decomposition of polyprodrugs. This pattern can avoid the toxic side effects of chemotherapy on normal tissues. HD-Micelles using inert bonds as a coupling agent showed poor efficacy in both cell lines. We speculate that although micelles have been shown to be effectively uptake by cells, HCPT molecules are fixed in the hard-to-degrade molecular chains, making it difficult to bind with enzymes and DNA.

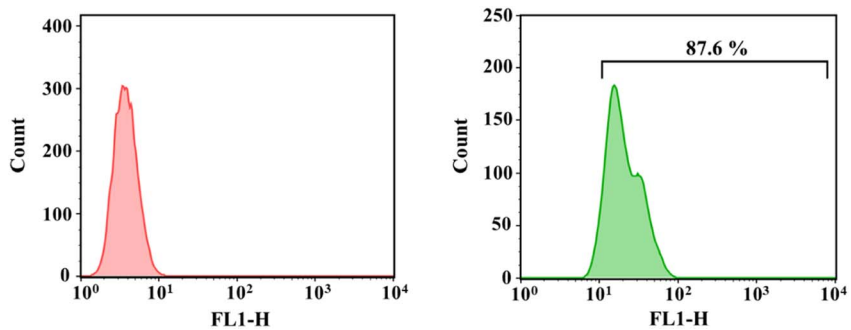

Fig. 6 Cellular internalization rate of TK-Micelle/pDNA complexes at N/P = 10 in 22RV1 cells.

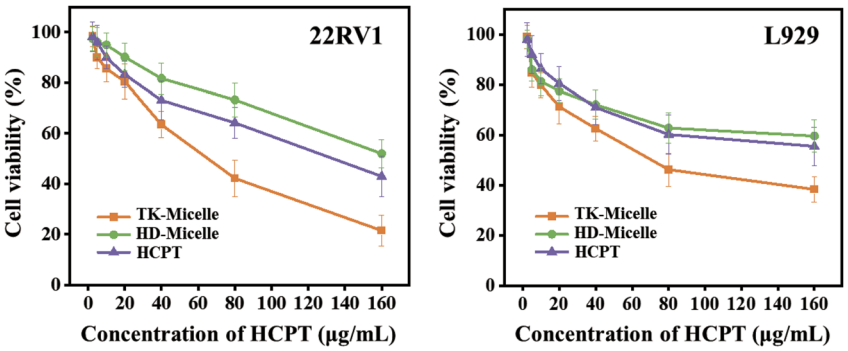

Fig. 7 The cytotoxicity of TK-Micelles, HD-Micelles, and free HCPT against 22RV1 and L929 cells. Mean ± s.d., $n = 6$.

In addition, polycations on the surface of micelles can also cause inevitable cytotoxicity. Dense positive charges will cause the formation of nanopores in the cell membrane, reduce the stability of the cell membrane, and then cause cytotoxicity.[34] The micelle prepared by using low molecular weight PEI, on the one hand, it was confirmed by agarose gel electrophoresis that it would not affect the condense property of the plasmid (Fig. 2), and it was confirmed by hemolysis experiment that the destruction to the cell membrane could be ignored. Moreover, the complexation of plasmids on the micellar surface can further reduce the cytotoxicity caused by cations.

In vitro gene transfection assay

For the purpose of accurately evaluating the transfection efficiency of micelles and avoiding the obvious cytotoxic effects of HCPT introduction on cells, we prepared a kind of micelle with a morphology similar to the TK-Micelle using polycaprolactone (PCL, as hydrophobic segments) and PEI (M_W = 1800 Da). The preparation steps are described in the ESI Materials.† As illustrated in Fig. 8a, in 22RV1 cells and L929 cells, the transfection efficiency shows a trend of first increasing and then decreasing with the rise of the N/P ratio. At the N/P = 15, all groups showed ideal transfection efficiency, and the ROS-responsive micelles showed higher transfection efficiency than non-responsive micelles. We consider that this is because when the N/P ratio is low, it is difficult for insufficient cations to form a compact and sufficient number of complexes with the plasmid. As the number of cations increases, the complex forms a size that is easily internalized by the cell until the optimal N/P ratio of 15 is reached. With the further increase of the N/P ratio, excessive cations will lead to cytotoxicity, as discussed above, resulting in cell death and decreased transfection efficiency. At the same N/P ratio, the transfection efficiency of micelle (PCL-TK-PEI) is greater than that of micelle (PCL-PEI). We speculate that the responsiveness of ROS is related to the faster escape of plasmids from the complex (consistent with the agarose gel electrophoresis), which is more pronounced in 22RV1 cells with high levels of ROS expression.

The pEGFP plasmid, as a reporter gene, can express green fluorescent protein, and green fluorescence can be observed under excitation. Therefore, we used cationic micelles to deliver pEGFP plasmid to visually observe the transfection ability of the samples (Fig. 8b). At the optimum N/P ratio, the number of positive cells treated with micelle (PCL-TK-PEI)/pEGFP and micelle (PCL-PEI)/pEGFP was significantly higher than that treated with PEI/pEGFP. The flow cytometry analysis showed that the number of positive cells in micelle (PCL-TK-PEI)/pEGFP group and micelle (PCL-PEI)/pEGFP group were 37(±3)% and 34(±3)% respectively, which were higher than the PEI/pEGFP group. It is concluded that the cationized micelle shell constructed by low molecular weight PEI can effectively deliver plasmids to cells. And the ROS-responsiveness improves the transfection efficiency of the carriers.

Antitumor effect of chemotherapy combined with suicide gene system

To evaluate the antitumor effect of the CD/5-FC suicide gene system in conjunction with chemotherapy, PEI/pCMV-CD, TK-Micelle/pCMV-CD, and HD-Micelle/pCMV-CD with the best N/P ratio were used to transport suicide genes (pCMV-CD) respectively, and the cytokilling activity with 5-FC at different concentrations was analyzed. As illustrated in Fig. 9a, when the concentrationof 5-FC reached 40 μg mL^{-1}, the cell viability of TK-Micelle/pCMV-CD treated cells was already lower than 20, and with the growth of 5-FC concentration, the cell viability continued to decrease but was no longer significant. This is the result of the collaboration between suicide genes and chemotherapeutic drugs. On the one hand, 5-FC was turned into 5-FU by cytosine deaminase to kill cells; on the other hand, HCPT released by micelles also kills cells simultaneously. The ability of two synergistic effects to kill tumor cells is superior to that of the micelle treated cells alone.

The combination of the suicide gene and chemotherapy to kill tumor cells was visualized by using double-staining of living and dead cells. Calcein-AM can move across the cell membrane and get rid of the AM group through esterase in viable cells. The resulting calcein will emit strong green fluorescence. PI (propyl iodide) can enter dead cells through damaged cell membranes and embed in the DNA to emit red fluorescence. As shown in Fig. 9b–d, when the fc concentration was 40, the PEI/pCMV-CD group showed an unsatisfactory cytokilling activity, while the cells treated by the TK-Micelle/pCMV-CD group showed the

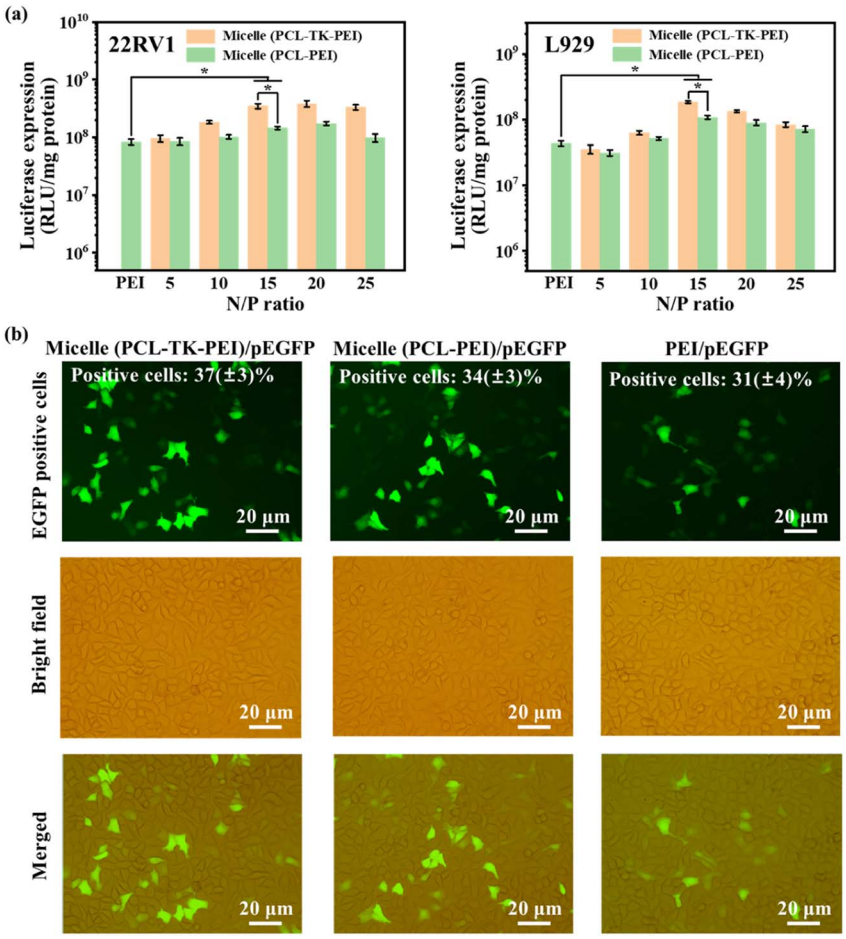

Fig. 8 (a) Luciferase gene expression mediated by the PEI (M_W = 25 000 Da, N/P = 10), micelle (PCL-TK-PEI), and micelle (PCL-PEI) in 22RV1 and L929 cells (mean ± SD, n = 3, *p < 0.05), and (b) typical photos of pEGFP expression mediated by micelle (PCL-TK-PEI), micelle (PCL-PEI), and PEI in 22RV1 cells.

largest number of red spots, indicating that plenty of cells were killed under the dual effects of suicide genes and chemotherapeutic drugs.

Experimental

Materials

1,1′-Carbonyldiimidazole, (CDI, 97%), hydroxycamptothecin (HCPT), branched polyethylenimine (PEI, M_w = 1800 Da), thioglycolic acid, 1,7-heptanediol, triphosgene, bismuth chloride, 2,2-dimethoxypropane, and lithium aluminium hydride, were purchased from Sigma-Aldrich Chemical (St. Louis, MO, USA). Hydrogen peroxide 30% aqueous solution, dimethyl sulfoxide (DMSO), acetonitrile, tetrahydrofuran (THF), dichloromethane (DCM), diethyl ether, and *N*,*N*-dimethylformamide (DMF), were purchased from Sinopharm Chemical Reagent Co., Ltd (China). 3-(4,5-Dimethylthiazol-2yl)-2,5-diphenyltetrazolium bromide (MTT), and 5-fluorocytosine were obtained from Aladdin Chemical Reagent Co., Ltd (China). Dulbecco's Modified Eagle's Medium (DMEM), Roswell Park Memorial Institute 1640 (RPMI-1640), fetal bovine serum (FBS), penicillinestreptomycin and trypsin were purchased from Genom Technology Co., Ltd (China).

Preparation and characterization of ROS-responsive polyprodrugs

The synthesis of the ROS-responsive coupling agent and the polyprodrugs (TK-pHCPT) was referred to in a previous report.[18] Nuclear magnetic resonances (NMR, Bruker ARX 300 MHz spectrometer, Rheinstetten, Germany) was used to determine the structure of compounds. The detailed synthetic route and structural characterization of the obtained compounds are provided in the ESI Materials.†

Preparation of amphiphilic copolymer (TK-pHCPT-PEI)

TK-pHCPT (200 mg, 0.05 mmol) were dispersed in 20 mL of THF. Then, CDI (1.62 mg, 0.01 mmol) was added. After stirring for 24 h, PEI (M_w = 1800 Da, 36 mg, 0.02 mmol) in 5 mL of methanol and 1.5 mL of triethylamine was added to the CDI-motivated TK-pHCPT solution. The mixed solution was continued to react for 24 h in a nitrogen atmosphere at 25 °C. The solution was concentrated by rotary evaporation and dialyzed (MWCO 7000) against deionized water. The amphiphilic copolymer was finally obtained after lyophilization.

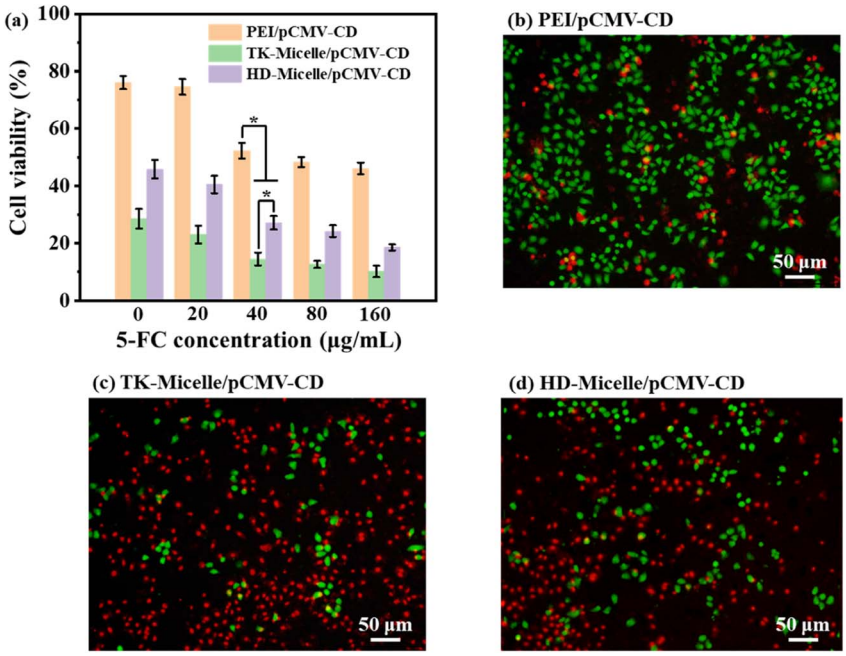

Fig. 9 (a) Cell viability of the 22RV1 cells served with different concentrations of 5-FC afterward transfection mediated by PEI/pCMV-CD (N/P = 10), TK-Micelle/pCMV-CD (N/P = 15), and HD-Micelle/pCMV-CD (N/P = 10) complexes (mean ± SD, $n = 6$, $*p < 0.05$). Double-staining of 22RV1 cells treated by (b) PEI/pCMV-CD, (c) TK-Micelle/pCMV-CD, and (d) HD-Micelle/pCMV-CD complexes at their optimal N/Ps in the existence of 5-FC (40 μg mL^{-1}).

Preparation of micelles and micelle/pDNA complexes

The TK-pHCPT-PEI (10 mg) was dissolved in 2 mL of methanol and the solution was added dropwise to 8 mL of PBS (pH = 7.4) solution under vigorously stirring. The formed TK-Micelle dispersion was concentrated by rotary evaporation to be ready for use.

The micelle and pDNA solutions with equal volumes were mixed to attain the planned N/P ratio to form micelle/pDNA complexes. Each mixture was permitted to stand for 30 min at room temperature before use.

Characterization of micelle/pDNA complexes

The capability of cationic micelles to compress the pDNA and the ability of complexes to controlled release the pDNA in the high concentration ROS solution were evaluated by agarose gel electrophoresis. Samples with series N/P ratios holding 0.2 μg of pDNA were prepared. Agarose (0.4 g) was dissolved in 40 mL of TAE running buffer (40 mM Tris-acetate, 1 mM EDTA). 4 μL of GelRed™ was added to the solution to stain the double-stranded DNA. The Sub-Cell system (Bio-Rad Labs, Richmond, CA, USA) was implemented for 30 min with a voltage of 110 V. The stained pDNA stripes were imaged with a UVP bioimaging system (BioDoc-It 220, UVP Inc. Upland, CA, USA). To evaluate the pDNA release-promoting effect of ROS, complexes with changed N/P ratios were incubated in an H_2O_2 solution with a concentration of 50 μM for an additional 30 min before being added to the gel.

The morphology of micelles and micelle/pDNA complexes (N/P = 15) was observed by TEM (JEM-2100, Jeol, Japan). Their particle size and zeta potential were measured by a laser particle size and zeta potential analyzer (Malvern Nano-ZS90, Southborough, MA, USA). Micelle/pDNA complexes with changed N/P ratios (5, 10, 15, 20) were prepared. Each solution (containing 3 μg pDNA) was diluted to 1 mL for testing. The stability of micelle particle size was continuously monitored in PBS for one week.

HCPT release profile

The TK-Micelle or HD-Micelle in 10 mL PBS was transferred to a dialysis tube (MWCO 3500). The dialysis tube was placed in an appropriate volume of PBS (pH = 7.4) with an H_2O_2 concentration of 50 μM. The ambient temperature was sustained at 37 °C, and 3 mL of the liquid was removed for testing at predetermined time points, while 3 mL of fresh PBS was supplemented. The quantity of HCPT in the extracted sample was determined by a UV spectrophotometer (UH4150 spectrometer, Japan) at 365 nm.

Hemolysis test

The RBCs were washed to supreme purity and then concentrated to a concentration of 2%. RBC suspensions were mixed with micelles, micelle/pDNA complexes, PBS, and Triton X-100 at different concentrations or N/P ratios. After incubation for 3 h at 37 °C, the suspensions were centrifuged (2000 rpm, 10 min) and the supernatants were collected. The absorbance of the supernatant at 545 nm was recorded by a UV spectrophotometer. The hemolysis rate was calculated according to the following formula: hemolysis rate (%) = $(A_{test} - A_{neg})/(A_{pos} - A_{neg}) \times 100\%$, where A_{test} is the absorbance value of the supernatant containing samples, A_{neg} is the absorbance value of PBS group, and A_{pos} is the absorbance value of the Triton X-100 group.

Cellular internalization

Cells were cultured according to standard procedures as detailed in the ESI Materials.† The plasmid (pRL-CMV) was first marked with a green molecular probe (YOYO-1) and then complexed with cationic micelles (N/P = 15). After 22RV1 cells were seeded in 6-well plates and cultured for 24 h, the already prepared complexes were added and the incubation continued for 4 h. The cells were then digested with trypsin, collected by centrifugation, and re-suspended in 1.5 mL of PBS. The fluorescence intensity of positive 22RV1 cells was detected using a flow cytometer (BD LSR II, BD, Franklin Lakes, NJ, USA).

In vitro cytotoxicity assay

22RV1 cells and L929 cells were seeded in 96-well plates (10 000 cells per well) and cultured according to standard conditions for 24 h. The medium was then exchanged with continuously diluted samples (micelles and free drugs) in fresh mediums. After another 24 h of culture, replace the old one with 100 μL of medium having MTT (0.5 mg mL^{-1}). After continuing the culture for 4 h, carefully discard the medium and add 100 microliters of DMSO. The absorbance at 490 nm is read by a microplate reader (Bio-Rad 680, Bio-Rad Labs, Richmond, CA, USA) after a short period of oscillation. The cell viability is calculated as stated by the following formula: cell viability (%) = $A_{sample}/A_{control} \times 100\%$, where A_{sample} and $A_{control}$ are the absorbance values of cells treated with samples and cells cultured in normal medium.

Evaluation of transfection efficiency

22RV1 cells and L929 cells were used to test the vector's ability to deliver genes. pRL-CMV plasmid encoding ranilla luciferase was adopted as a reporter gene. The cells were seeded in 24-well plates (50 000 cells per well) and incubated under standard conditions for 24 h. Replace the old culture medium with 300 μL of medium (accompanied by 10% FBS) containing the sample with different N/Ps (1.0 μg of pDNA in each well). After 4 h, remove the culture medium and add 500 μL of fresh medium (10% FBS). After continuing to incubate for 20 h, gently wash the cells with PBS and then add 100 μL of lysis reagent to each well. According to the method of the renilla luciferase reporter gene assay kit (Beyotime Biotechnology, Shanghai, China), the luminescence intensity of the sample was determined using a luminometer (Berthold Lumat LB 9507, Berthold Technology, Bad Wilbad, Germany) and the protein content was examined.

22RV1 cells were used to evaluate the number of cells labeled with enhanced green fluorescent protein (EGFP). Complexes were prepared by combining plasmid pEGFP with micelles (N/P = 15) or PEI (N/P = 10). The cell culture process is similar to the above steps. After transfection, fluorescence microscopy (Leica DMI3000B, Wetzlar, Germany) was used to observe and record the green production of cells using a blue filter, and a BD LSR II flow cytometer (BD Biosciences, San Jose, CA, USA) was applied to evaluate the proportion of EGFP-positive cells.

In vitro antitumor activity

22RV1 cells were seeded in 96-well plates and cultured for 24 h. A fresh medium containing the complex (TK-Micelle/pCMV-CD and HD-Micelle/pCMV-CD at N/P = 15; PEI/pCMV-CD at N/P = 10) was added subsequently. After 4 h of transfection, replace the old medium with fresh medium containing different concentrations (0–160 mg mL^{-1}) of 5-FC. 72 h later, the cell viability of cells after different sample treatments was assessed by MTT assay.

The survival status of the cells was evaluated visually by double-staining of living and dead cells. X cells were seeded in 24-well plates and cultured for 24 h. The old medium was then exchanged with a medium having suicide gene complexes (at optimal N/P ratio, containing 1.0 μg pCMV-CD). After 4 h of transfection, replace with culture medium containing 5-FC (40 μg mL^{-1}). Incubation for another 72 h, cells were stained as stated by the instructions of the live/dead cell double-staining kit. Fluorescent photographs are taken using a fluorescence microscope.

Statistical analysis

Relevant data are conveyed as means ± standard deviation (mean ± SD). The student's t-test was applied for statistical analysis. When $p < 0.05$, the difference was identified as significant. Each experiment was conducted at least three times.

Conclusions

We developed a co-delivery system that can deliver chemotherapeutic drugs and suicide genes at once. The ROS-responsive polyprodrug was prepared using HCPT, and the cationic shell of the micelle was used to deliver the CD suicide gene. The use of low molecular weight PEI reduces cytotoxicity while maintaining considerable nucleic acid compression capacity. Based on the controllable release triggered by the high concentration of ROS in tumor cells, it avoids killing and damaging normal cells. In PC cell lines, it has been confirmed that transient expression of suicide genes can kill tumor cells through bystander effects. This combination of chemotherapy and gene therapy has shown promising therapeutic effects on PC.

Author contributions

Kai Li: conceptualization, formal analysis, data curation, and writing – original draft; Sinan Tian: formal analysis, investigation, and data curation; Ke Sun and Qingguo Su: validation, data curation, and visualization; Yanhui Mei: conceptualization, validation, and funding acquisition; Wenjie Niu: conceptualization, validation, supervision, and project administration.

Conflicts of interest

There are no conflicts to declare.

Acknowledgements

This work was supported by the Science and Technology Innovation Policy Guidance Plan of Binzhou (2023SHZ039). Parts of Fig. 1 and graphical abstract were created with **https://www.biorender.com/**.

Notes and references

1 M. Sekhoacha, K. Riet, P. Motloung, L. Gumenku, A. Adegoke and S. Mashele, Prostate cancer review: genetics, diagnosis, treatment options, and alternative approaches, *Molecules*, 2022, **27**, 5730.

2 J. Cuzick, M. A. Thorat, G. Andriole, O. W. Brawley, P. H. Brown, Z. Culig, R. Eeles, L. Ford, F. Hamdy, L. Holmberg, D. Ilić, T. Key, C. la Vecchia, H. Lilja, M. Marberger, F. Meyskens, L. Minasian, C. Parker, H. Parnes, S. Perner, H. Rittenhouse, J. Schalken, H. Schmid, B. Schmitz-Dräger, F. Schröder, A. Stenzl, B. Tombal, T. Wilt and A. Wolk, Prevention and early detection of prostate cancer, *Lancet Oncol.*, 2014, **15**, e484–e492.

3 R. J. Rebello, C. Oing, K. E. Knudsen, S. Loeb, D. C. Johnson, R. E. Reiter, S. Gillessen, T. Van der Kwast and R. G. Bristow, Prostate cancer, *Nat. Rev. Dis. Primers*, 2021, **7**, 9.

4 K. Komura, C. J. Sweeney, T. Inamoto, N. Ibuki, H. Azuma and P. W. Kantoff, Current treatment strategies for advanced prostate cancer, *Int. J. Urol.*, 2018, **25**, 220–231.

5 M. S. Litwin and H. J. Tan, The diagnosis and treatment of prostate cancer a review, *JAMA, J. Am. Med. Assoc.*, 2017, **317**, 2532–2542.

6 P. Posdzich, C. Darr, T. Hilser, M. Wahl, K. Herrmann, B. Hadaschik and V. Grünwald, Metastatic prostate cancer-a review of current treatment options and promising new approaches, *Cancers*, 2023, **15**, 461.

7 R. P. Huben and G. P. Murphy, A comparison of diethylstilbestrol or orchiectomy with buserelin and with methotrexate plus diethylstilbestrol or orchiectomy in newly diagnosed patients with clinical stage D2 cancer of the prostate, *Cancer*, 1988, **62**, 1881–1887.

8 T. Nelius, K. Rinard and S. Filleur, Oral/metronomic cyclophosphamide-based chemotherapy as option for patients with castration-refractory prostate cancer – review of the literature, *Cancer Treat. Rev.*, 2011, **37**, 444–455.

9 C. Manogue, W. Fleming, E. Ledet, E. Jaeger, J. Layton, P. Barata, B. Lewis and O. Sartor, Continuous IV infusion of 5-flourouracil in heavily pretreated metastatic castrate-resistant prostate cancer, *Clin. Genitourin. Cancer*, 2022, **20**, 586–590.

10 S. M. N. Abdel-Hafez, R. A. Rifaai and W. Y. Abdelzaher, Possible protective effect of royal jelly against cyclophosphamide induced prostatic damage in male albino rats; a biochemical, histological and immuno-histochemical study, *Biomed. Pharmacother.*, 2017, **90**, 15–23.

11 M. A. Moyad and M. Roach, Promoting wellness for patients on androgen deprivation therapy: why using numerous drugs for drug side effects should not be first-line treatment, *Urol. Clin. North Am.*, 2011, **38**, 303–312.

12 S. Adepu and S. Ramakrishna, Controlled drug delivery systems: current status and future directions, *Molecules*, 2021, **26**, 5905.

13 M. R. Donthi, S. R. Munnangi, K. V. Krishna, R. N. Saha, G. Singhvi and S. K. Dubey, Nanoemulgel: a novel nano carrier as a tool for topical drug delivery, *Pharmaceutics*, 2023, **15**, 164.

14 Y. Liu, B. J. Yue, R. R. Wang, H. L. Cong, H. Hu, B. Yu and Y. Q. Shen, Photothermal-responsive prussian blue nanocages loaded with thrombin for tumor starvation therapy and photothermal therapy, *Biomater. Sci.*, 2023, **11**, 4938–4947.

15 X. M. Cheng, J. Gao, Y. Ding, Y. Lu, Q. C. Wei, D. Z. Cui, J. L. Fan, X. M. Li, E. Zhu, Y. N. Lu, Q. Wu, L. Li and W. Huang, Multi-functional liposome: a powerful theranostic nano-platform enhancing photodynamic therapy, *Adv. Sci.*, 2021, **8**, 2100876.

16 Y. Zhang, Q. S. Wang, T. Ma, D. W. Zhu, T. J. Liu and F. Lv, Tumor targeted combination therapy mediated by functional macrophages under fluorescence imaging guidance, *J. Controlled Release*, 2020, **328**, 127–140.

17 L. S. Jabr-Milane, L. E. van Vlerken, S. Yadav and M. M. Amiji, Multi-functional nanocarriers to overcome tumor drug resistance, *Cancer Treat. Rev.*, 2008, **34**, 592–602.

18 Q. Y. Meng, H. Hu, X. D. Jing, Y. Sun, L. P. Zhou, Y. W. Zhu, B. Yu, H. L. Cong and Y. Q. Shen, A modular ROS-responsive platform co-delivered by 10-hydroxycamptothecin and dexamethasone for cancer treatment, *J. Controlled Release*, 2021, **340**, 102–113.

19 Y. Sun, Q. M. Wu, Q. Y. Fu, H. L. Cong, Y. Q. Shen, B. Yu and H. Hu, Reactive oxygen species-responsive polyprodrug micelles deliver cell cycle regulators for chemosensitization, *Talanta*, 2024, **267**, 125242.

20 Q. M. Wu, Y. Hu, B. Yu, H. Hu and F. J. Xu, Polysaccharide-based tumor microenvironment-responsive drug delivery systems for cancer therapy, *J. Controlled Release*, 2023, **362**, 19–43.

21 M. Choi, A. M. Jazani, J. K. Oh and S. M. Noh, Perfluorocarbon nanodroplets for dual delivery with ultrasound/GSH-responsive release of model drug and passive release of nitric oxide, *Polymers*, 2022, **14**, 2240.

22 Y. Y. Wang, X. X. Wang, R. S. Xie, J. C. Burger, Y. Tong and S. Q. Gong, Overcoming the blood–brain barrier for gene therapy *via* systemic administration of GSH-responsive silica nanocapsules, *Adv. Mater.*, 2023, **35**, 2208018.

23 L. Naldini, Gene therapy returns to centre stage, *Nature*, 2015, **526**, 351–360.

24 Y. Cao, Y. F. Tan, Y. S. Wong, M. W. J. Liew and S. Venkatraman, Recent advances in chitosan-based carriers for gene delivery, *Mar. Drugs*, 2019, **17**, 381.

25 C. N. Xu, H. Y. Tian and X. S. Chen, Recent progress in cationic polymeric gene carriers for cancer therapy, *Sci. China: Chem.*, 2017, **60**, 319–328.

26 U. Bezeljak, Cancer gene therapy goes viral: viral vector platforms come of age, *Radiol. Oncol.*, 2022, **56**, 1–13.

27 S. Duarte, G. Carle, H. Faneca, M. C. P. de Lima and V. Pierrefite-Carle, Suicide gene therapy in cancer: where do we stand now?, *Cancer Lett.*, 2012, **324**, 160–170.
28 I. Yoshimura, S. Suzuki, T. Tadakuma and M. Hayakawa, Suicide gene therapy on LNCaP human prostate cancer cells, *Int. J. Urol.*, 2001, **8**, S5–S8.
29 S. Vodenkova, T. Buchler, K. Cervena, V. Veskrnova, P. Vodicka and V. Vymetalkova, 5-Fluorouracil and other fluoropyrimidines in colorectal cancer: past, present and future, *Pharmacol. Ther.*, 2020, **206**, 107447.
30 C. Sethy and C. N. Kundu, 5-Fluorouracil (5-FU) resistance and the new strategy to enhance the sensitivity against cancer: implication of DNA repair inhibition, *Biomed. Pharmacother.*, 2021, **137**, 111285.
31 Z. Z. Xu, G. B. Shen, X. Y. Xia, X. Y. Zhao, P. Zhang, H. H. Wu, Q. F. Guo, Z. Y. Qian, Y. Q. Wei and S. F. Liang, Comparisons of three polyethyleneimine-derived nanoparticles as a gene therapy delivery system for renal cell carcinoma, *J. Transl. Med.*, 2011, **9**, 46.
32 C. J. Richards, T. C. Q. Burgers, R. Vlijm, W. H. Roos and C. Aberg, Rapid internalization of nanoparticles by human cells at the single particle level, *ACS Nano*, 2023, **17**, 16517–16529.
33 Y. L. Tu, X. Xiao, Y. S. Dong, J. S. Li, Y. Liu, Q. Y. Zong and Y. Y. Yuan, Cinnamaldehyde-based poly(thioacetal): a ROS-awakened self-amplifying degradable polymer for enhanced cancer immunotherapy, *Biomaterials*, 2022, **289**, 121795.
34 I. R. C. Hill, M. C. Garnett, F. Bignotti and S. S. Davis, In vitro cytotoxicity of poly(amidoamine)s: relevance to DNA delivery, *Biochim. Biophys. Acta, Gen. Subj.*, 1999, **1427**, 161–174.
35 X. Zhang, Y. J. Duan, D. F. Wang and F. L. Bian, Preparation of arginine modified PEI-conjugated chitosan copolymer for DNA delivery, *Carbohydr. Polym.*, 2015, **122**, 53–59.
36 Q. Tang, F. L. Ji, W. H. Sun, J. Y. Wang, J. L. Guo, L. Y. Guo, Y. C. Li and Y. M. Bao, Combination of baicalein and 10-hydroxy camptothecin exerts remarkable synergetic anti-cancer effects, *Phytomedicine*, 2016, **23**, 1778–1786.